Electronic Structure of Carbon Nanotubes

The discovery of the tubule form of the graphite sheet has attracted enormous attention over the last decade because of its fundamental and technological interests. The formation of the carbon nanotube (CNT) by chemical vapor deposition using transition-metal (TM) as catalysts has been investigated extensively. The TM catalysts were proposed to come into contact with tube walls and significantly influenced the transport and electronic properties. The curvature of the graphite sheet was among one of the factors considered to explain the change of the electronic states in CNTs. Since tips have a smaller radius of curvature, the local electronic structures at tips were proposed to be different from those of sidewalls. We try to improve the understanding of CNTs by performing X-ray absorption near edge structure (XANES) measurements for CNTs catalyzed by Fe layers with various CNT diameters. Furthermore, we combine angle-dependent C *K*-edge XANES and scanning photoelectron microscopy (SPEM) measurements for highly aligned CNT's to better understand the enhancement of density of state (DOS) and the mechanism of electron field emission at the tips.

The CNTs were prepared on the *p*-type Si(100) substrate by microwave plasma enhanced chemical vapor deposition (MPE-CVD). Prior to the MPE-CVD process, thin layers of Fe with various thickness were deposited on the Si substrate by e-beam evaporation. Using the scanning electron microscopy (SEM), the randomly oriented multi-walled CNTs prepared with the 30,150, and 300 A Fe layers were observed to be around 10 μm in length and 10 $\pm$5 nm, 30 $\pm$15 nm, and 220 $\pm$100 nm in diameter, respectively. In addition, the vertically aligned CNTs were also prepared on the *p*-type Si substrates by MPE-CVD. Using the SEM and transmission electron microscopy, the well-aligned multi-walled CNTs were observed to be approximately 7 μm long and 10-20 nm in diameter, as shown in Fig. 1.

Fig. 2 displays the C *K*-edge XANES spectra of graphite and three randomly oriented multi-walled CNTs prepared with three different CNT diameters. The general line shapes in the C *K*-edge XANES spectra of the three CNTs and graphite appear to be similar regardless of the different diameters of the CNTs. The two prominent peaks near 285.7 and 292.7 eV are known to be associated with the unoccupied π^* and σ^* bands, respectively. Between the π^* and σ^* peaks, a

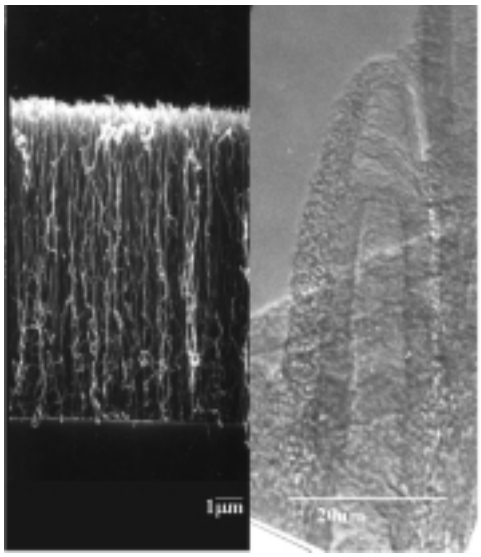

Fig. 1: (a) Scanning electron microscope image and (b) transmission electron microscope image of the well-aligned multiwalled carbon nanotubes with diameters of 10-20 nm.

weak feature (labeled by a vertical solid line) near 287.5 eV is also observed. This feature was attributed to free-electron-like interlayer states in the graphite. Another weak peak appears around 283.5 eV (labeled by a vertical dashed line) and was previously attributed to a defect electronic state of the disordered carbon in diamond films. The inset of Fig.2 illustrates the relative intensities of the π^*-, σ^*-band and the interlayer-state features for the three CNTs. The intensities of the π^*-band and interlayer-state features are clearly enhanced relative to those of the graphite. Since the intensities of these features are approximately proportional to the density of the unoccupied C 2*p*-derived states, the increased intensities of these features can be correlated with the increased numbers of unoccupied C 2*p* orbitals or a charge transfer from the C 2*p* to Fe 3*d* orbitals. The intensities of the near-edge features increase with the decrease of the CNT diameter, which suggest that the C 2*p* orbitals in the smaller-diameter CNTs may lose more charge to the 3*d* orbitals of the catalyzing Fe atoms than that of the larger-diameter CNTs.

Fig. 3 displays the normalized Fe $L_{3,2}$-edge XANES spectra of the Fe metal and the three CNTs with different diameters. According to dipole-transition selection rules, the dominant transition is from Fe $2p_{3/2}$ and $2p_{1/2}$ to the unoccupied Fe 3*d* states. In Fig. 3 the shapes of the Fe $L_{3,2}$-edge XANES spectra of CNTs differ significantly from that of the pure Fe metal. The intensities of the CNT white-line features are also significantly smaller than that of pure Fe. (The intensity of the Fe spectrum has been scaled by a factor of 1/2). To understand the dependence of charge transfer between C and Fe atoms on the curvature of the graphite sheet in CNTs, the intensities of the white-line features $I(L_3)$ at the Fe L_3-edge are illustrated in the inset of Fig. 3. $I(L_3)$ is determined by subtracting the background intensity described by an arctangent function, as indicated by the dashed-line in Fig. 3. $I(L_3)$ for CNTs are clearly seen to be significantly lower than that for pure Fe. $I(L_3)$ gradually increases with the diameter of the carbon tube, suggesting that the number of unoccupied Fe 3*d*-derived states increases with the increase of the nanotube diameter, since $I(L_3)$ is approximately proportional

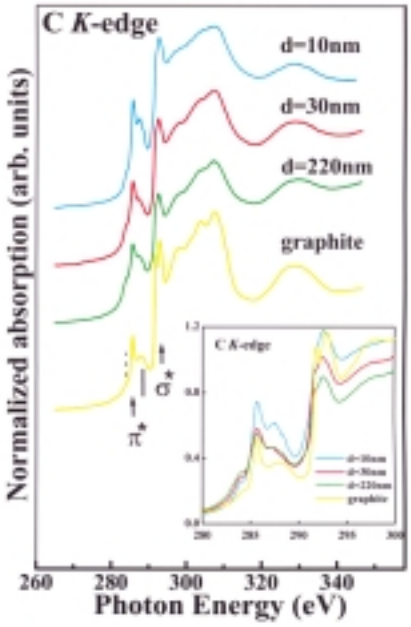

Fig. 2: Normalized C K-edge absorption spectra of (a) graphite and carbon nanotubes with diameters of (b) 220 ±100 nm, (c) 30 ±15 nm, and (d) 10 ±5 nm. The inset displays the enlarged part of the near-edge in a magnified scale.

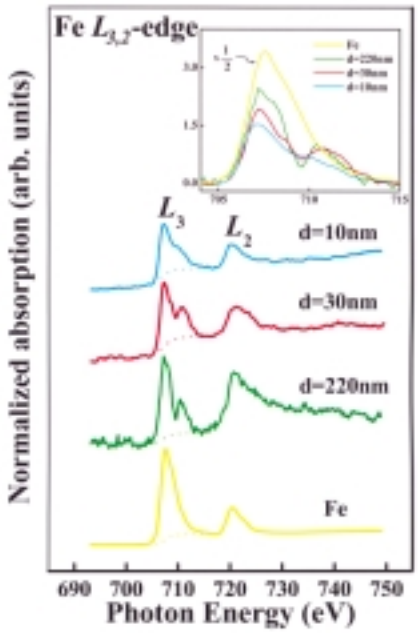

Fig. 3: Normalized Fe $L_{3,2}$ near-edge absorption spectra of (a) the Fe metal and the carbon nanotubes with diameters of (b) 220±100 nm, (c) 30±15 nm, and (d) 10±5 nm. The dashed line represents the extrapolated background at the Fe L_3-edge. The center of the continuum step of the arctangent function was selected at the maximum-height of the white-line features. The white-line region of the Fe L_3-edge is shown in the inset in a magnified scale.

to the density of the unoccupied Fe 3*d*-derived states. In other words, the 3*d* orbitals of the Fe atoms in contact with the smaller-diameter CNT may gain more charge from the carbon 2*p* orbitals than those in contact with the larger-diameter CNT. This result is consistent with that of the C *K*-edge XANES spectra.

Fig. 4 shows the angle-dependent C *K*-edge XANES spectra of the well-aligned multi-walled CNTs with 10-20 nm in diameter. The general line shapes of the C *K*-edge XANES spectra obtained with different angles of incidence θ, between the surface normal and the incident synchrotron radiation appear to be similar, though their intensities are different. The inset in the lower part of Fig. 4 shows that the intensities of the π^*- and σ^*-band features of the aligned CNTs increases from $\theta = 72°$ to 0°. Since the intensity is approximately proportional to the density of the unoccupied C 2*p*-derived states, the result indicates an increase of the absorption intensity with the decrease of θ not only for the unoccupied π^* states but also for the σ^* state. The CNTs are highly aligned, therefore the spectra obtained at normal incidence ($\theta = 0°$) and at large incident angle ($\theta = 72°$) can be expected to be dominated by contributions from tips and sidewalls, respectively. Thus, our C *K*-edge XANES result shows that the density of states (DOSs) of both unoccupied π^* and σ^* bands are enhanced at the tips.

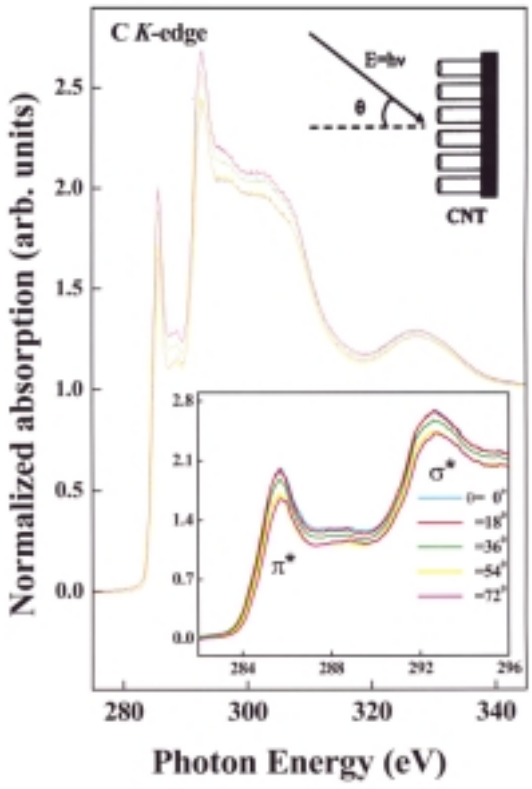

Fig. 4: Normalized C K-edge absorption spectra of the aligned carbon nanotubes as a function of θ. The inset shows an enlarged part of the near-edge spectra.

Fig. 5 shows the SPEM image of the C 1*s* photoelectrons emitted from the cross-section of aligned CNTs. Although due to the limited resolution of SPEM, individual tubes could not be resolved, nanotube bundles can be clearly distinguished in the SPEM image. The C 1*s* photoelectrons have maximum intensity in the tip region marked by A. In the sidewall region below the tip region, there are some less bright regions marked by B, which may contain bent or shorter CNTs. The dark sidewall region marked by C exhibits a shadowing effect. The image of tips is clearly much brighter than that of the rest part of the CNTs. To elucidate the local electronic structures of different regions, we have plotted valence-band and C 1*s* photoemission spectra originated from A, B, and C regions in Figs. 6(a) and (b), respectively. Fig. 6(a) shows that the tips have a larger valence-band DOS over the whole energy range plotted. Our result is different to previous SPEM measurements by Suzuki *et al.*, (ELETTRA Highlights 2000 - 2001, p. 68 - 69), which showed the enhancement of tip DOS only near E_f. Fig. 6(b) shows that the intensity of region B is not larger than that of region C, though Fig. 5 shows that it is brighter. Fig. 6(b) also shows that the tips have a higher C 1*s* core-level intensity. The C 1*s* spectrum of the tip apparently shifts toward a higher binding energy by ~0.2 eV relative to those of the sidewall spectra. The tip valence band spectra showed a smooth and uniform increase in intensity over a wide energy range but no sharp

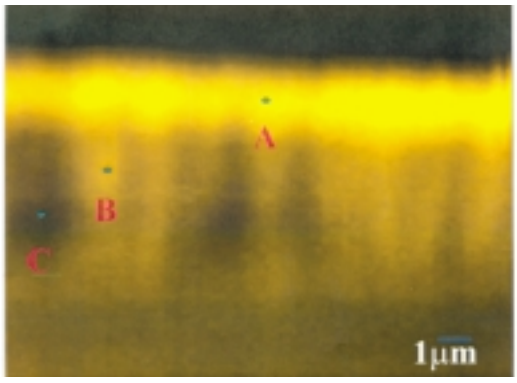

Fig. 5: The cross-sectional SPEM C 1s image of aligned CNTs.

resonance. The SPEM results indicate a larger DOSs for the tip region. The enhancement of the DOSs from localized states at the tip is presumably determined by the local atomic configuration, e.g., curvature, defects, chirality and the enhanced semiconducting character.

In summary, we have investigated the local electronic structures of Fe-catalyzed and randomly oriented CNTs with various diameters. The intensities of π^*- and σ^*-band and interlayer-state features in the C *K*-edge XANES spectra of these CNTs vary with the diameter of the CNT. Using a combination of angle-dependent XANES and SPEM measurements for both unoccupied and occupied bands, respectively, we have studied the local electronic structures at the tips and sidewalls of highly aligned CNTs. We find that the intensities of π^*- and σ^*-band C *K*-edge XANES features are enhanced at the tip over an energy range larger than 10eV. The valence-band SPEM spectra also show that the tips have larger DOS's than sidewalls over an energy range larger than 10eV. This new finding can be attributed to the natural narrowing of the energy bands associated with the curvature, defects, chirality and enhanced semiconducting character at the tips.

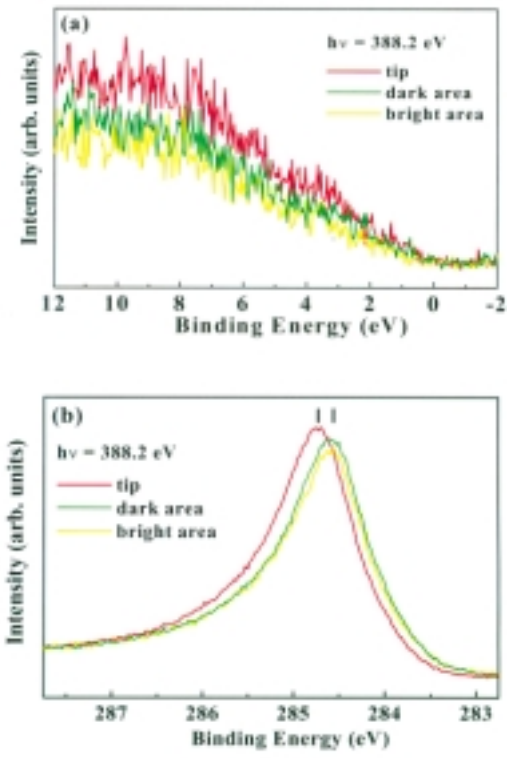

Fig. 6: (a) Valence-band spectra and (b) C 1s photoemission spectra from the three selected regions marked by A, B, and C shown in Fig. 4, which correspond to tip, bright area and dark area, respectively.

Beamlines:

09A1 U5 beamline

20A1 HSGM beamline

Experimental Stations:

SPEM end station

XANES end station

Authors:

W. F. Pong

Department of Physics, Tamkang University, Tamsui, Taiwan

M.-H. Tsai

Department of Physics, National Sun Yat-sen University, Kaohsiung, Taiwan

I.-H. Hong and R. Klauser

Synchrotron Radiation Research Center, Hsinchu, Taiwan

K. H. Chen

Institute of Atomic and Molecular Science, Academia Sinica, Taipei, Taiwan

L. C. Chen and T. J. Chuang

Center for Condensed Matter Sciences, National Taiwan University, Taipei, Taiwan

Publications:

- C. L. Yueh, J. C. Jan, J. W. Chiou, W. F. Pong, M.-H. Tsai, Y. K. Chang, Y. Y. Chen, J. F. Lee, P. K. Tseng, S. L. Wei, C. Y. Wen, L. C. Chen, and K. H. Chen, Appl. Phys. Lett. **79**, 3179 (2001).
- J. W. Chiou, C. L. Yueh, J. C. Jan, H. M. Tsai, W. F. Pong, I.-H. Hong, R. Klauser, M.-H Tsai,Y. K. Chang, Y. Y. Chen, C. T. Wu, K. H. Chen, S. L. Wei, C. Y. Wen, L. C. Chen, and T. J. Chuang (submitted).

Contact e-mail:

wfpong@mail.tku.edu.tw